$\bar{P}$ Production Measurements at the Fermilab Antiproton Source*

Stephen C. O'Day

Frank M. Bieniosek

Fermilab

P.O. Box 500 Batavia,IL 60510

Abstract

The Fermilab Antiproton Source has been used recently to provide $\bar{p}$s for $p - \bar{p}$ collider experiments. Measurements of the $\bar{p}$ yield per proton on target have been made and the data has been used as input for a pbar production model. Model predictions and data are presented for the $\bar{p}$ yield dependence on proton beam spot size using target thickness, lithium collection lens magnetic field gradient and lens current pulse phase. Planned improvements to the Antiproton Source target station are also discussed in this report.

1 INTRODUCTION

The principal components of the Fermilab Antiproton Source Target Station are the target secondary emissions monitor(TSEM)[1], target stack, lithium collection lens[2] and single turn pulsed magnet[3]. A 120 GeV beam of 2.0×10^{12} protons per pulse impinges on a nickel target. The transverse spot size is .12mm (horizontal) by .20mm (vertical) as measured by the TSEM. Secondaries are collected by the lithium lens and focused. A single turn pulsed magnet delivers a 3° kick to the 8.9 GeV/c beam which directs it into a beamline leading to the Debuncher ring.

Intensities after the construction of the Main Injector are expected to be high enough to melt the Ni production target[4] with the present proton beam spot size. Melting the target has been demonstrated to lower the yield in a Re target by 8% and to cause the release of airborne radionucleides[5]. A similar result is expected in Ni for melting point intensity on target. A system is currently being built which will sweep a highly focused proton beam in a circle on the target and then unsweep the secondaries[6] so that little or no yield is lost. In order to determine the final design parameters and expected $\bar{p}$ yield once this system is implemented, a measurement of yield into the debuncher as a function of spot position has been made. Using a Monte Carlo simulation (MCLENS)[7] of the production and collection of $\bar{p}$s, this data is used to predict the yield as a function of spot size, the Twiss parameters at the target and the combined aperture of the Debuncher and beamline leading to it.

2 YIELD VS. SPOT POSITION MEASUREMENTS

2.1 Yield in the Debuncher Transport Beamline

Using the TSEM which has 125 μm wire spacing, the position of the beam was located precisely in the horizontal transverse direction. The horizontal spot location is varied by changing the field in a horizontal dipole magnet upstream of the target. The beam was located at several vertical points and interpolation was made based on readback from the upstream vertical dipole magnet which controls the vertical spot location.

The yield into the Debuncher Transport beamline was determined by a toroid at location 704(TOR704) and an ion chamber at location 728(IC728) (see figure 1). The antiproton portion of the measured intensity at these locations is completely obscured by the presence of pions and electrons which are present in roughly equal proportion. Note that the decay length for charged pions at 8.9 GeV is 500 meters. This is approximately the distance from the target to the resistive wall monitor. The circumference of the Debuncher ring is also 500 meters.
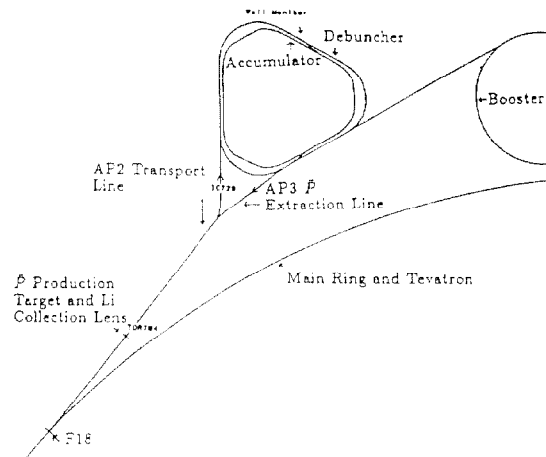

Figure 1. The Fermilab Antiproton Source.

2.2 Yield in the Debuncher Ring

The yield on the first turn was measured using the Debuncher resistive wall monitor. The circulating antiproton yield was measured using a digital signal analyzer. The signal analyzer does a fast Fourier transform of the longitudinal Schottky power spectrum and integrates it over a specified bandwidth. The output is calibrated to a d.c.

current transformer.

3 MCLENS ANALYSIS

3.1 Debuncher Transport Beamline Aperture

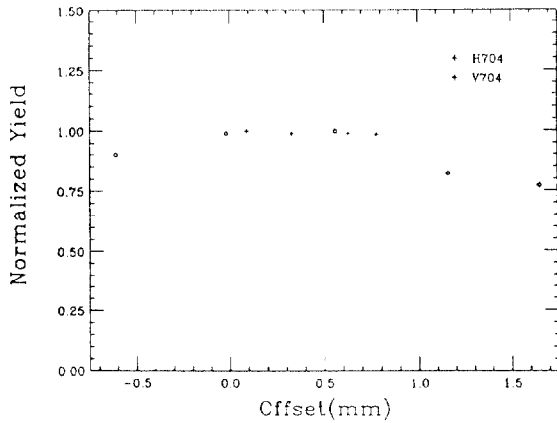The horizontal and vertical data for TOR704 are shown in figure 2.

Figure 2. Horizontal Secondary Yield.

The lens to target distance is 21.5cm for these. The yield vs. spot size horizontal data for IC728 are shown for different lens to target distances in figure 3.
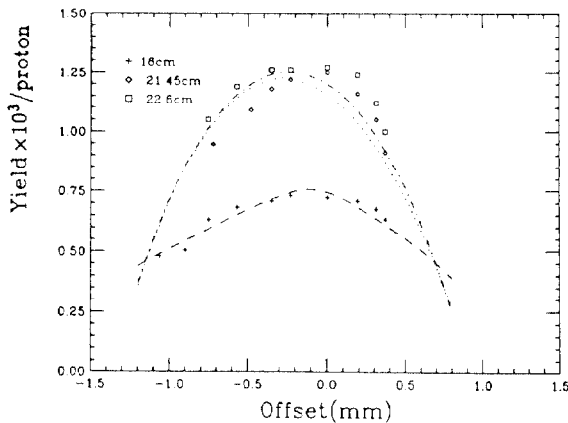

Figure 3. Horizontal IC728 Secondary Yield for Different $Z_{lens-target}$

Corresponding data for the Debuncher are shown in figure 4. The MCLENS program provides the fitted curves for each plot using the values shown in table 1. Based on the best fit admittances, it can be seen that the aperture drops from an unnormalized emittance of 40πmm-mRad at TOR704 to 30πmm-mRad at IC728 to 17π in the Debuncher for the horizontal data. Note that the Debuncher horizontal and vertical apertures have been measured independently to be typically between 22 and 27πmm-mRad. The data imply the presence of a horizontal aperture restriction in the Debuncher injection line. The error on the
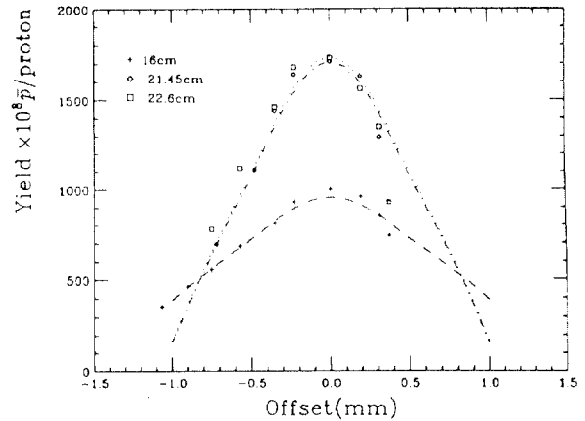
stated admittances is $\pm 3\pi$mm-mRad.

Figure 4. Horizontal Debuncher Secondary Yield for Different $Z_{lens-target}$

Table 1: MCLENS Parameters

| Parameter	Value
Lens Radius(m)	.01
Lens Length(m)	.16
Lens to Target Distance(m)	.17
Target Disk Radius(m)	.06
Target Material	Xf
Target Size(m)	.02
β Central $p(GeV/c)$	8.86
β $\sigma_p(GeV/c)$	.176
Half-Angle of Primary Production(rad)	.07
Half-Angle of Secondary Production(rad)	.1
Proton Beam $\sigma_x = \sigma_y(m)$	.00016
TOR704 Horizontal Admittance ($\pi mm - mRad$)	40
TOR704 Vertical Admittance($\pi mm - mRad$)	40
IC728 Horizontal Admittance ($\pi mm - mRad$)	30
IC728 Vertical Admittance($\pi mm - mRad$)	40
Debuncher Horizontal Admittance ($\pi mm - mRad$)	17
Debuncher Vertical Admittance($\pi mm - mRad$)	22
α_x at Lens(Rad)	0.0
β_x at Lens(m)	1.5
α_y at Lens(Rad)	0.0
β_y at Lens(m)	1.5
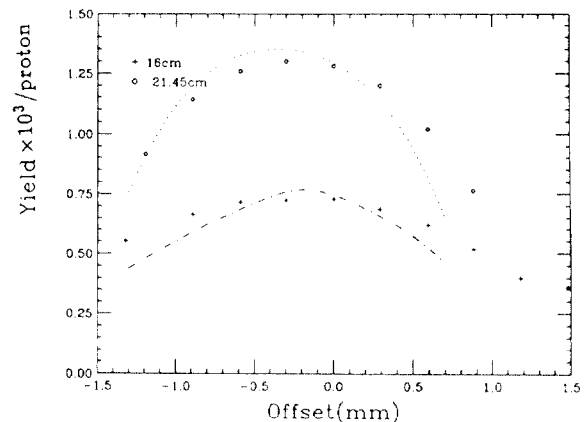
Figure 5. Vertical IC728 Secondary Yield for Different $Z_{lens-target}$

The vertical data shown in figures 5 and 6 are consistent with a 40π mm-mRad aperture up to IC728 and a 23πmm-
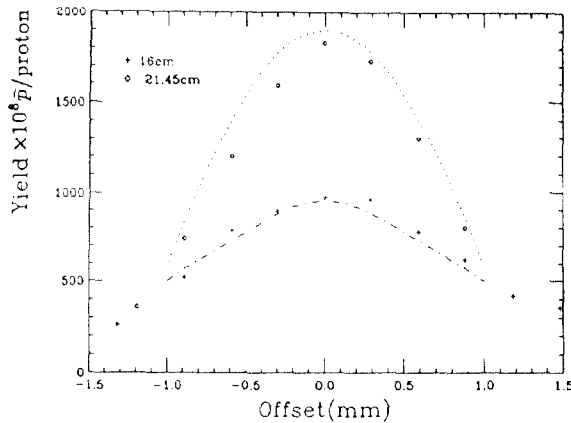
2439

mRad Debuncher aperture.

Figure 6. Vertical Debuncher Secondary Yield for Different $Z_{lens-target}$

3.2 Yield vs. Spot Size Calculation and Measurement

Gormley[8] measured yield vs. spot size directly using a TSEM with twice the wire to wire spacing of the present TSEM. The sem profile was fit to a Gaussian and the yield into the Debuncher was recorded for each spot size. The spot size was increased by reducing quadrupole strengths in the focusing section of the proton beamline just upstream of the target.

The yield vs. spot position data presented in section 3.1 has been integrated to give a prediction of the yield vs. spot size. The data from both measurements are presented in figure 7 and are in good agreement.
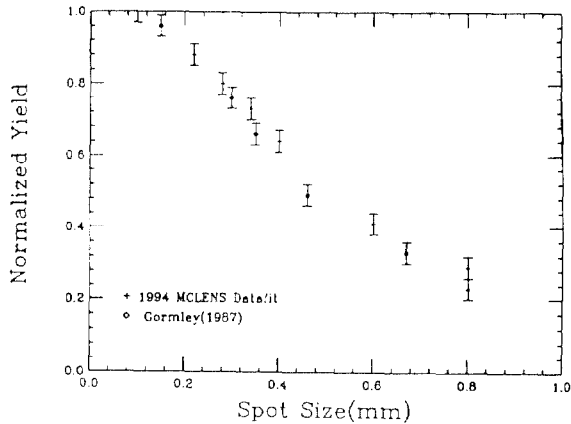

Figure 7. $\bar{P}$ Yield vs. Spot Size.

3.3 Implications for Target Survival

A conservative estimate of spot size without target sweeping would try to maintain or reduce the present energy deposition density. Although the energy deposition threshold for stress wave fractures is not well known[9] it is clear that energy deposition density decreases with increasing spot size. Thus, a larger spot size is better for target survival.

The maximum energy deposition is proportional to $\sigma^{-1.35}$ for Cu. Using this dependence for Ni (which is similar to Cu in atomic weight, number and mass density), the present .16mm spot size should be scaled by $2.5^{1/1.35}$ since the Main Injector intensity is predicted to be 2.5 times the present intensity. The resulting spot size is .32mm. The sweeping system design assumes a .1mm beam spot which results from the introduction of a lithium focusing lens 2m upstream of the target. The effective spot size would then be $\sqrt{(.33^2 + .1^2)} = .35$mm. The $\bar{p}$ yield without sweeping for $\sigma_{beam} = .35$mm is 75% of the yield at $\sigma_{beam} = .1$mm. Sweeping increases this fraction to 95%- a 27% gain.

4 SUMMARY

The Debuncher and Debuncher transport beamline apertures as well as the Twiss parameters were obtained by optimizing the MCLENS fit to yield vs. spot position data. The yield vs. spot size curve was obtained by integration. The need for a sweeping system in antiproton production at Main Injector intensities was verified.

5 REFERENCES

[1] P. Hurh, S. O'Day, R. Dombrowski and T. Page " A 10μm Resolution Secondary Emission Monitor for Fermilab's Targeting Station", in Proceedings of the 1993 Particle Accelerator Conference , Washington D.C., May 17-20 1993, pp. 2459-2461.

[2] G. Dugan. et. al.,"Mechanical and electrical design of the Fermilab lithium lens and transformer system",IEEE Trans. Nucl. Sci. 30,1983,pp. 3660.

[3] P. Hurh, M. Gormley, J. Hangst and S. O'Day " A Radiation-Hardened Pulsed Magnet for the Tevatron-I Target Station", in Proceedings of the 1993 Particle Accelerator Conference,San Francisco, California, May 6-9 1991, pp. 2361-2363.

[4] C. Bhat, N. Mokhov,"Calculation of Beam Sweeping Effect for the Fermilab Antiproton Source",Fermilab-TM-1585,1989.

[5] S. O'Day, F. Bieniosek and Kris Anderson" New Target Results from the FNAL Antiproton Source", in Proceedings of the 1993 Particle Accelerator Conference , Washington D.C., May 17-20 1993, pp. 3096-3099.

[6] F. Bieniosek, "A Beam Sweeping System for the Fermilab Antiproton Production Target", Fermilab-TM-1857,1993.

[7] S. O'Day and F. Bieniosek,"8.9 GeV $\bar{P}$ Yield Measurements at the Fermilab Antiproton Source",Nuclear Instruments and Methods A343,1994, pp. 343-350.

[8] M. Gormley,"Target Station Upgrade",Antiproton Source internal memo,1988.

[9] Z. Tang, K. Anderson,"Shock Waves in $\bar{p}$ Targets", Fermilab TM-1763,1991.